Estimation of Time-Domain Calibration Parameters to Restore MIMO-TDD Channel Reciprocity

Boris Kouassi[1], Irfan Ghauri[2] and Luc Deneire[1]
[1]Laboratoire I3S, Sophia Antipolis, France
[2]Intel Mobile Communications, Sophia Antipolis, France
Email: kouassi@i3s.unice.fr, irfan.ghauri@intel.com, deneire@i3s.unice.fr

***Abstract*—Spatial interweave cognitive radio opportunistically exploits spatial holes to enable transmission of secondary systems. The latter form carefully aligned spatial beams so that there is no interference to the primary system. This requires acquisition of the (spatio-temporal) channel state (CS) between the secondary emitter and the primary receiver. CS can be acquired by using a multi-input multi-output time-division-duplex (MIMO-TDD) setup thanks to channel reciprocity inherent in such systems. Unfortunately, global reciprocity is often jeopardized by the nonreciprocal radio frequency front-ends (RF) at the two ends of the link. Restoration of reciprocity to compensate for the RF calls for on-line (and hence low complexity) calibration parameters estimation. In this paper, we propose an approach to estimate the space-time-domain parameters restoring the channel reciprocity in a frequency selective MIMO-TDD context. Accounting for antenna coupling effects, we find accurate space-time-domain calibration parameters and demonstrate real-time calibration process in an OFDM system[1].**

***Index Terms*—Interweave cognitive radio, reciprocity calibration, MIMO/TDD, beamforming, frequency selective channel estimate, precoding.**

I. Introduction

The emergence of multiple wireless communication systems in the last decade causes an overcrowding of the radio spectrum, spurring research in innovative radio transmission techniques like cognitive radio (CR). CR enables coexistence of secondary (unlicensed) systems with primary licensed systems in the same radio environment. More precisely, CR opportunistically exploits the radio environment information (spectral occupancy, number of users, etc) to improve secondary transmissions, while avoiding the disruption of primary transmissions [2]. In [3], the authors classify cognitive radio as *overlay, underlay, and interweave*. Interweave CR, subject of this work, exploits white spaces (unused dimensions or *holes*) in the radio environment to fit secondary transmission. Depending upon the communications context, these holes may exist in any dimension: temporal, spatial, frequency. This paper addresses *spatial* interweave, an approach also taken in [4] and [5], where the secondary transmission occurs under the assumption of channel reciprocity in a multi-input multi-output time division duplex (MIMO-TDD) system. In this scenario, reciprocity between uplink and downlink is exploited to perform beamforming. In practice, however, the overall channel including emitter (Tx) and receiver (Rx) filters is not reciprocal due to the radio frequency (RF) front-ends circuitry [4] [6] causing breakdown of the most fundamental assumption needed for Tx beamformer design.

Focusing on Orthogonal Frequency Division Multiplexing (OFDM) systems, where the frequency selective channel in the frequency domain can be seen as a number of parallel flat fading channels [7], authors have proposed calibration parameter estimation methods in the frequency domain (see [4] [8] and references therein). For OFDM systems with a large number of carriers, this method leads to large complexity. One way to tackle the complexity concern is to develop low complexity methods in the frequency domain [9]. In [10] and [11] the calibration problem is simplified assuming that calibration matrices are diagonal, which implies no antenna mutual coupling.

In this paper, we propose estimation of calibration parameters in the time domain, thus generalizing the calibration process to other transmission systems. Moreover, the number of parameters in the time domain is much lower than the number of parameters in the frequency domain for large OFDM systems, hence leading to lower complexity methods. The proposed approach exploits the block Toeplitz structure of the time-domain MIMO channel matrices to determine calibration parameters, and helps formulation of a structured total least-squares (TLS) problem [12] [13]. Solving the TLS problem calibration matrices are recovered even under antenna coupling assumption (non-diagonal calibration matrices). We compare the performance with usual calibration techniques in OFDM systems [4].

This paper is structured as follows: Section II describes the system model and describes the assumptions under which our investigations are made. In Section III we present the proposed time-domain calibration technique. Section IV shows the evaluation framework and the simulation results. We present complexity comparison of time- and frequency-domain methods in section V. Finally, section VI draws conclusions of this work.

Notations : The notations in Table I are used throughout this paper.

[1]This work in part shows results presented at the real-time cognitive radio demonstration of the European project FP7 CROWN (Cognitive Radio Oriented Wireless Networks) [1].

CROWNCOM 2012, June 18-20, Stockholm, Sweden

DOI 10.4108/icst.crowncom.2012.248472

Table I: notations

Symbol	*Description*
c	Complex or real scalar
$\mathbf{v}$	Complex or real vector
$\mathbf{M}$	Complex or real matrix
$\mathbf{M}^T$	Transpose of $\mathbf{M}$
$*$	Convolution
$\otimes$	Kronecker product
$vec(\mathbf{M})$	Vectorization of matrix $\mathbf{M}$
$\mathbf{FT}\{\mathbf{M}(\tau)\} = \mathbf{M}(\nu)$	Discrete Fourier transform of matrix $\mathbf{M}(\tau)$
$\mathbf{FT}^{-1}\{\mathbf{M}(\nu)\}$	The inverse Fourier transform of matrix $\mathbf{M}(\nu)$

II. System model

Fig. 1 shows goings-on in a MIMO frequency selective channel assuming L different paths with N_A antennas at the Tx side (A), and N_B antennas at the Rx side (B). The multipath propagation is due to the reflection, diffraction and scattering phenomenons caused by objects between the transmitter and the receiver.

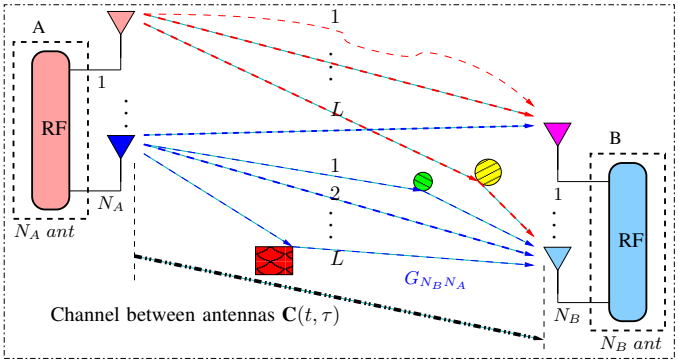

Fig. 1. Multipath MIMO system.

The overall MIMO multipath channel between antennas $\mathbf{C}(t,\tau)$ is a $N_B \times N_A$ matrix expressed by equation (1). The received signal $\mathbf{y}(t) \in \mathbb{C}^{N_B \times 1}$ at the node B is defined by

$$\mathbf{y}(t) = \begin{bmatrix} y_1(t) \\ \vdots \\ y_{N_B}(t) \end{bmatrix} = \mathbf{C}(t,\tau) * \mathbf{x}(t) + \mathbf{n}(t), \quad (1)$$

$$\mathbf{C}(t,\tau) = \begin{bmatrix} \mathbf{c}_{11}(t,\tau) & \cdots & \mathbf{c}_{1N_A}(t,\tau) \\ \vdots & \ddots & \vdots \\ \mathbf{c}_{N_B1}(t,\tau) & \cdots & \mathbf{c}_{N_BN_A}(t,\tau) \end{bmatrix}, \mathbf{x}(t) = \begin{bmatrix} x_1(t) \\ \vdots \\ x_{N_A}(t) \end{bmatrix}$$

where $\mathbf{c}_{ij}^T(t,\tau) = [c_{ij}(t,0), \cdots, c_{ij}(t,L-1)]$, with $\mathbf{x}(t) \in \mathbb{C}^{N_A \times 1}$ the vector transmitted by N_A antennas, $\mathbf{n}(t) \in \mathbb{C}^{N_B \times 1}$ the additive white Gaussian noise (AWGN) introduced by the receiver, and τ the delay generated by L multipaths. The received signal at the i^{th} antenna of node B is defined by:

$$y_i(t) = \sum_{j=1}^{N_A} \{\mathbf{c}_{ij}(t,\tau) * x_j(t)\} + n_i(t) \quad (2)$$

where $x_j(t)$ is the stream transmitted by the j^{th} antenna, and $n_i(t)$ the AWGN introduced at the i^{th} receiver antenna. The MIMO architecture including the RF front-ends and the multipath channel can be summarized in Fig. 2.

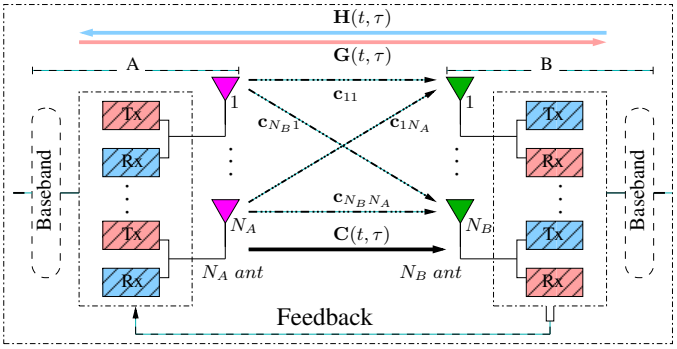

Fig. 2. Description of the transmit (Tx) and the receive (Rx) RF filters in a MIMO-TDD system.

Assuming that the RF front-ends are also frequency selective and denoted respectively $\mathbf{R}_{X_A}(t,\tau)$, $\mathbf{T}_{X_A}(t,\tau)$ the transmit and the receive filters at side A and $\mathbf{R}_{X_B}(t,\tau)$, $\mathbf{T}_{X_B}(t,\tau)$ the filters at side B, the overall time domain channel $\mathbf{H}(t,\tau)$ from B to A and $\mathbf{G}(t,\tau)$ from A to B (see Fig. 2) are defined by:

$$\mathbf{H}(t,\tau) = \mathbf{R}_{X_A}(t,\tau) * \mathbf{C}^T(t,\tau) * \mathbf{T}_{X_B}(t,\tau), \quad (3)$$

$$\mathbf{G}(t,\tau) = \mathbf{R}_{X_B}(t,\tau) * \mathbf{C}(t,\tau) * \mathbf{T}_{X_A}(t,\tau), \quad (4)$$

where $\mathbf{C}(t,\tau)$ is the electromagnetic channel between antennas, $\mathbf{R}_{X_A}(t,\tau)$, $\mathbf{T}_{X_A}(t,\tau)$ the square matrices of dimension $N_A \times N_A$ and $\mathbf{R}_{X_B}(t,\tau)$, $\mathbf{T}_{X_B}(t,\tau)$ the square matrices of dimension $N_B \times N_B$. As mentioned in [6], the RF front-ends depend on the electronic components and are assumed to be time-invariant. Finally, from equations (3) and (4) we write:

$$\mathbf{G}(t,\tau) = \mathbf{P}_{X_B}(\tau) * \mathbf{H}^T(t,\tau) * \mathbf{P}_{X_A}(\tau), \quad (5)$$

assuming that $\mathbf{P}_{X_B}(\tau) = \mathbf{FT}^{-1}\{\mathbf{P}_{X_B}(\nu)\}$ with $\mathbf{P}_{X_B}(\nu) = \mathbf{R}_{X_B}(\nu)\mathbf{T}_{X_B}^{-T}(\nu)$, and $\mathbf{P}_{X_A}(\nu) = \mathbf{R}_{X_A}^{-T}(\nu)\mathbf{T}_{X_A}(\nu)$ the RF filters in frequency domain. This relation allows to write:

$$\mathbf{P}_{X_B}^{-1}(\nu)\mathbf{G}(t,\nu) = \mathbf{H}^T(t,\nu)\mathbf{P}_{X_A}(\nu), \quad (6)$$

and the time domain representation of equation (6) is expressed by:

$$\mathbf{Q}(\tau) * \mathbf{G}(t,\tau) = \mathbf{H}^T(t,\tau) * \mathbf{P}(\tau) \quad (7)$$

with $\mathbf{Q}(\tau) = \mathbf{FT}^{-1}\{\mathbf{P}_{X_B}^{-1}(\nu)\}, \mathbf{P}(\tau) = \mathbf{FT}^{-1}\{\mathbf{P}_{X_A}(\nu)\}$. Our objective is now to find the calibration parameters $\mathbf{Q}(\tau)$ and $\mathbf{P}(\tau)$ enabling restoration of the frequency selective channel reciprocity. To achieve this goal, we use a relative calibration technique [6]. The relative calibration does not require a third-party calibration device as opposed to absolute calibration techniques. It simply observes the channel state information (CSI) in a first observation phase, exchanges observations of the CSI between the two ends of the link and derives the calibration factors using the CSI observed. The next section addresses algorithms for relative calibration.

III. Time-domain Calibration

In order to determine the calibration factors in time domain, we reformulate equation (7) as a matrix multiplication using block Toeplitz matrices. For a given time t, we infer the relations (8) and (9) for each element of channel matrices:

$$\mathbf{q}_{ii}(\tau) * \mathbf{g}_{ii}(t,\tau) = \mathbf{T}_{\mathbf{Q}ii}[\tau]\mathbf{g}_{ii}(t,\tau) \quad (8)$$

$$\mathbf{h}_{ii}(t,\tau) * \mathbf{p}_{ii}(\tau) = \mathbf{T}_{\mathbf{H}ii}(t,\tau)\mathbf{p}_{ii}(\tau), \quad (9)$$

with $\mathbf{g}_{ii}(t,\tau) \in \mathbb{C}^{L\times 1}$ the elements of $\mathbf{G}(t,\tau)$ such as:

$$\mathbf{G}(t,\tau) = \begin{bmatrix} \mathbf{g}_{11}(t,\tau) & \cdots & \mathbf{g}_{1N_A}(t,\tau) \\ \vdots & \ddots & \vdots \\ \mathbf{g}_{N_B1}(t,\tau) & \cdots & \mathbf{g}_{N_BN_A}(t,\tau) \end{bmatrix}, \quad (10)$$

where L is the length of the channel $\mathbf{G}(t,\tau)$, idem for $\mathbf{h}_{ii}(t,\tau)$, $\mathbf{q}_{ii}(\tau)$ and $\mathbf{p}_{ii}(\tau)$ respectively the elements of matrices $\mathbf{H}(t,\tau)$, $\mathbf{Q}(\tau)$ and $\mathbf{P}(\tau)$. $\mathbf{T}_{\mathbf{Q}ii}[\tau]$ and $\mathbf{T}_{\mathbf{H}ii}(t,\tau)$ are Toeplitz structured as:

$$\mathbf{T}_{\mathbf{Q}ii}[\tau] = \underbrace{\left.\begin{bmatrix} \mathbf{q}_{ii}(0) & \mathbf{q}_{ii}(-1) & \cdots & \mathbf{q}_{ii}(1-L) \\ \mathbf{q}_{ii}(1) & \mathbf{q}_{ii}(0) & \cdots & \mathbf{q}_{ii}(2-L) \\ \vdots & \ddots & \vdots & \vdots \\ \mathbf{q}_{ii}(M-1) & \mathbf{q}_{ii}(M-2) & \cdots & \mathbf{q}_{ii}(M-L) \end{bmatrix}\right\}_{rows}^{M}}_{L\ columns} \quad (11)$$

Assuming that the RF filters have the same length Lp, $M = L + Lp - 1$, $\mathbf{q}_{ii}(\tau) \in \mathbb{C}^{M+L+1}$ ($\mathbf{q}_{ii}(\tau) = 0$ for $\tau < 0$), finally we write the block Toeplitz matrix $\mathbf{B}_{\mathbf{Q}}[\tau]$:

$$\mathbf{B}_{\mathbf{Q}}[\tau] = \begin{bmatrix} \mathbf{T}_{\mathbf{Q}11}[\tau] & \cdots & \mathbf{T}_{\mathbf{Q}1N_A}[\tau] \\ \vdots & \ddots & \vdots \\ \mathbf{T}_{\mathbf{Q}N_B1}[\tau] & \cdots & \mathbf{T}_{\mathbf{Q}N_BN_A}[\tau] \end{bmatrix}, \quad (12)$$

$\mathbf{B}_{\mathbf{H}}(t,\tau)$ and $\mathbf{T}_{\mathbf{H}ii}(t,\tau)$ are defined in the same manner, then we recast equation (7) such as :

$$\mathbf{B}_{\mathbf{Q}}[\tau]\mathbf{G}(t,\tau) = \mathbf{B}_{\mathbf{H}}(t,\tau)\mathbf{P}(\tau). \quad (13)$$

Finally, we need to find $\mathbf{B}_{\mathbf{Q}}[\tau]$ and $\mathbf{P}(\tau)$. To this end, we determine $\mathbf{B}_{\mathbf{Q}}[\tau]$ and $\mathbf{P}(\tau)$ minimizing the following distance:

$$\underset{\{\mathbf{B}_{\mathbf{Q}}[\tau],\mathbf{P}(\tau)\}}{\operatorname{argmin}} ||\mathbf{B}_{\mathbf{Q}}[\tau]\mathbf{G}(t,\tau) - \mathbf{B}_{\mathbf{H}}(t,\tau)\mathbf{P}(\tau)||_F^2, \quad (14)$$

which is equivalent to:

$$\underset{\{\mathbf{B}_{\mathbf{Q}}[\tau],\mathbf{P}(\tau)\}}{\operatorname{argmin}} ||vec(\mathbf{B}_{\mathbf{Q}}[\tau]\mathbf{G}(t,\tau)) - vec(\mathbf{B}_{\mathbf{H}}(t,\tau)\mathbf{P}(\tau))||^2.$$

From the relation:

$$vec(A_{M\times N}B_{N\times P}) = (B^T \otimes \mathbf{I}_M)vec(A) = (\mathbf{I}_P \otimes A)vec(B),$$

we write:

$$vec(\mathbf{B}_{\mathbf{Q}}[\tau]\mathbf{G}(t,\tau)) - vec(\mathbf{B}_{\mathbf{H}}(t,\tau)\mathbf{P}(\tau)) = \quad (15)$$

$$(\mathbf{G}^T(t,\tau) \otimes \mathbf{I}_{MN_B})vec(\mathbf{B}_{\mathbf{Q}}[\tau]) - (\mathbf{I}_{N_A} \otimes \mathbf{B}_{\mathbf{H}}(t,\tau))vec(\mathbf{P}(\tau)).$$

Hence, a solution to equation (14) is to find $\mathbf{B}_{\mathbf{Q}}[\tau]$ and $\mathbf{P}(\tau)$ such that:

$$\mathbf{Z}_{(MN_AN_B)\times(LMN_B^2+LpN_A^2)}\mathbf{C}_{(LMN_B^2+LpN_A^2)\times 1} = \mathbf{0}_{(MN_AN_B)\times 1}, \quad (16)$$

where

$$\mathbf{Z} = \begin{bmatrix} (\mathbf{G}^T(t,\tau)_{N_A\times LN_B} \otimes \mathbf{I}_{MN_B}) & -(\mathbf{I}_{N_A} \otimes \mathbf{B}_{\mathbf{H}}(t,\tau)_{MN_B\times LpN_A}) \end{bmatrix}$$

$$\mathbf{C} = \begin{bmatrix} vec(\mathbf{B}_{\mathbf{Q}}[\tau]) \\ vec(\mathbf{P}(\tau)) \end{bmatrix}. \quad (17)$$

We observe that it is possible to find the calibration parameters $\mathbf{C}$, if the number of rows in $\mathbf{Z}$ is greater than the number of rows in $\mathbf{C}$. In order to satisfy this condition, we use K channel measurements over the time such as: $\mathbf{Z_K} = [\mathbf{Z}^1, ..., \mathbf{Z}^K]^T$, then the concatenation of these measurements yields the relation $KMN_AN_B > (LMN_B^2 + LpN_A^2)$, for $K > (L\frac{N_B}{N_A} + Lp\frac{N_A}{MN_B})$ leading to

$$\begin{bmatrix} \mathbf{Z}^1 \\ \vdots \\ \mathbf{Z}^K \end{bmatrix} \mathbf{C} = \mathbf{0}; \quad (18)$$

$$\mathbf{Z_K}_{(KMN_AN_B)\times(LMN_B^2+LpN_A^2)}\mathbf{C}_{(LMN_B^2+LpN_A^2)\times 1} = \mathbf{0}_{(KMN_AN_B)\times 1}$$

Due to the channel estimation error, we acquire a noisy version of the real MIMO channel. Consequently, in (16) we introduce a model perturbation on $\mathbf{Z}$, leading to the following total least squares (TLS) problem:

$$\underset{\{\mathbf{C},\mathbf{\Delta Z_K}\}}{\operatorname{argmin}} ||\mathbf{\Delta Z_K}||_F \text{ s.t } (\mathbf{Z_K} + \mathbf{\Delta Z_K})\mathbf{C} = \mathbf{0}_{(KMN_AN_B)\times 1}. \quad (19)$$

Given the singular value decomposition (SVD) of $\mathbf{Z_K}$:

$$\mathbf{Z_K} = \mathbf{UDV}^H, \quad (20)$$

and writing $\mathbf{V}$ like an orthogonal basis consisting of the $\mathbf{Z_K}$ right singular vectors. The TLS solution of equation (19) lies in the last column of $\mathbf{V}$ and is given by:

$$\hat{\mathbf{C}} = -\mathbf{V}_{(LMN_B^2+LpN_A^2)}\mathbf{V}^{-1}_{\{(LMN_B^2+LpN_A^2),(LMN_B^2+LpN_A^2)\}}, \quad (21)$$

where $\mathbf{V}_{(LMN_B^2+LpN_A^2)}$ represents the last column vector of $\mathbf{V}$ and assuming $\mathbf{V}_{\{(LMN_B^2+LpN_A^2),(LMN_B^2+LpN_A^2)\}}$ the non singular element in the matrix $\mathbf{V}$ corresponding to the row $(LMN_B^2 + LpN_A^2)$ and column $(LMN_B^2 + LpN_A^2)$ (see [12]).

IV. Simulation framework and Results

The first simulation consists of estimating the calibration parameters with the proposed calibration technique, then the performance is compared to a calibration algorithm in frequency domain defined in [4], [9]. From a previous study [4], we select $K = 15$ channel estimations, to evaluate the reverse channel reconstruction reliability. Unlike previous calibrations studies [11], the simulations are done assuming crosstalk between antennas. Accordingly, the RF front-ends and calibration matrices ($\mathbf{R}, \mathbf{T}, \mathbf{P}$ equation (4) and (5)) are not diagonal.

Without loss of generality, we assume a 2×2 MIMO system ($N_A = N_B = 2$), the synthetic channel is supposed to be frequency selective with $L = 4$ multipaths with a fading following a Rayleigh distribution.

The algorithms are evaluated through the normalized mean square error (MSE) in the reconstructed channel: $\frac{||\mathbf{G}-\hat{\mathbf{G}}||_F^2}{||\mathbf{G}||_F^2}$

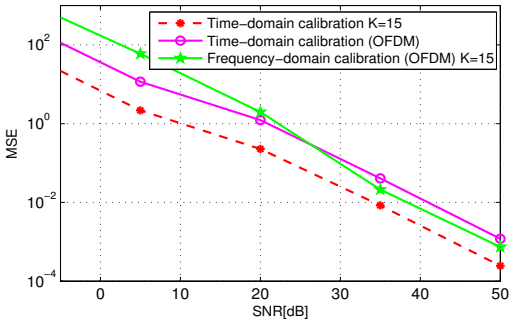

Fig. 3. The mean square error according to the SNR, showing the estimated calibration parameters in time-domain and in frequency domain.

Fig. 3 shows the reconstruction of calibration parameters using the time-domain estimation method. We use $K = 15$ channel estimations for the algorithms in frequency-domain and in time-domain. The performance of the two methods is equivalent. Fig. 3 also compares the performance of the MIMO-OFDM calibration across the subcarriers and the discrete Fourier transform (DFT) of the reconstruction through the new time-domain calibration. Even if the MIMO-OFDM technique outperforms the time-domain method in high SNR region, we observe that we are able to restore the channel reciprocity using our time-domain algorithm in the OFDM system considered.

Subsequently, in order to evaluate the performance of calibrated channels in beamforming, we design a simple transmit zero-forcing (Tx-ZF) precoding scheme using the calibrated channel. This can be written as

$$\mathbf{P_{Tx}} = \hat{\mathbf{G}}^{-1}, \tag{22}$$

where $\mathbf{P_{Tx}}$ defines the precoder, and $\hat{\mathbf{G}}$ the downlink channel estimated at the base station through reciprocity (Fig .4). Different techniques are addressed to design the precoder in a proposed OFDM system with 512 subcarriers and a QPSK (quadrature phase shift keying) modulation.

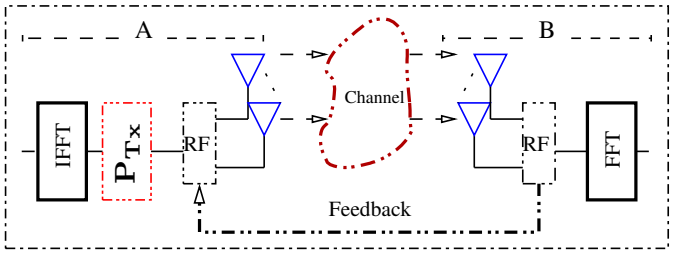

Fig. 4. OFDM transmission system, using a precoder and calibration procedure.

Assuming a first transmission step consisting of training sequence where the user estimates the channel with an estimation error defined by: $C_e \sim \mathcal{N}(0, \sigma_C^2 \mathbf{I})$.

Fig. 5 and Fig. 6 show the performance (bit error rate: BER) of the precoding scheme in a calibrated system. In a perfectly reciprocal channel, the use of the estimated channel transpose

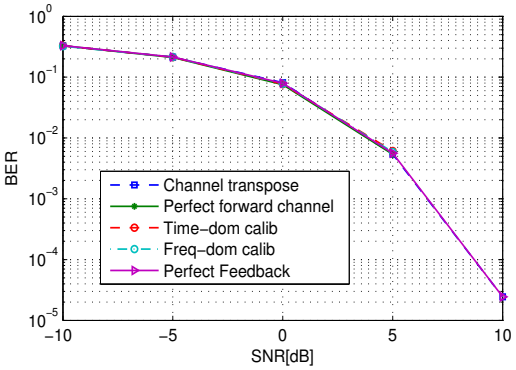

Fig. 5. The BER according to the SNR, describing the results in a perfect reciprocal MIMO channel, and the variance of channel estimation error $\sigma_C^2 = 10^{-3}$.

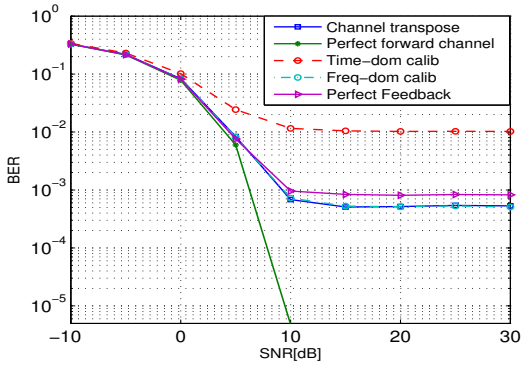

Fig. 6. Illustration of the BER according to the SNR, describing the results in a perfect reciprocal MIMO channel, and the variance of channel estimation error $\sigma_C^2 = 10^{-1}$.

($\mathbf{H}^T$) in the precoder, gives the same results as the perfect feedback case.

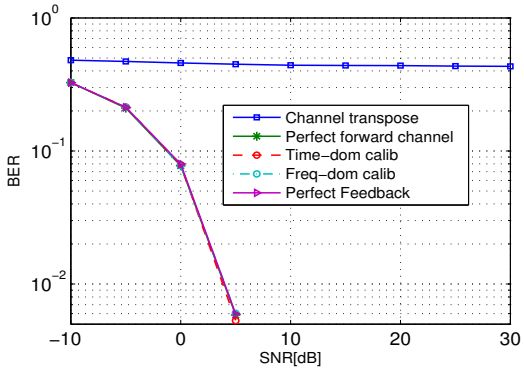

Fig. 7. The BER against the SNR, describing the results in a non-reciprocal MIMO channel, with crosstalk between antennas and $\sigma_C^2 = 10^{-3}$.

Fig. 7 illustrates the results when the channel is non-reciprocal and $\sigma_C^2 = 10^{-3}$. The bit error rate with the precoder using the estimated channel transpose collapses. This plot reveals the necessity of calibration: the time-domain and frequency-domain calibration algorithms show good BER

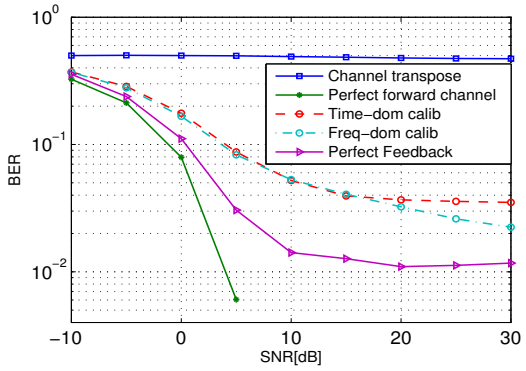

Fig. 8. The BER according to the SNR, describing the results in a non-reciprocal MIMO channel, with crosstalk between antennas and $\sigma_C^2 = 10^{-1}$.

performance, and the time-domain calibration result is close to the perfect feedback BER. Thus calibrated uplink channel for downlink beamforming can efficiently replace a system where the CSI is explicitly fed back.

We observe also that the impact of the channel estimation error is relevant in the estimation of reliable calibration parameters, as illustrated in Fig. 8 where the variance of the estimated channel is: $\sigma_C^2 = 10^{-1}$.

V. Complexity of the calibration procedure

In the sequel, the complexity comparison is based on the number of required operations ($O(min(NM^2, MN^2))$ flops) to perform the singular value decomposition of a matrix defined by M rows and N columns [14].

The dimension of the matrix in the time-domain calibration is $N_A.2M \times (N_B.L.2M + 2.Lp.N_A)$, and in the frequency-domain for one subcarrier $N_A.N_B \times (N_B^2 + N_A^2)$.

We observe that for a given channel with L multipaths in a $N_B \times N_A$ MIMO system, the complexity of the calibration in frequency domain will increase according to the number of subcarriers, as described in Fig. 9.

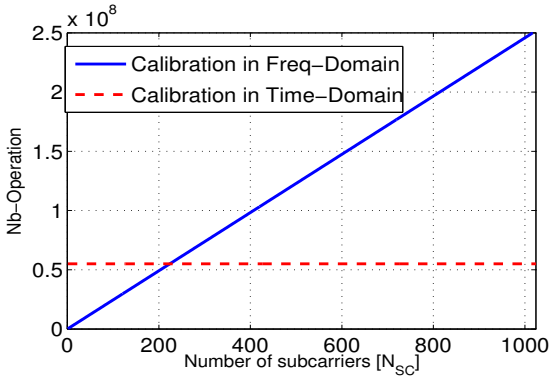

Fig. 9. Illustration of the computational complexity in a 4×4 MIMO system, $L = Lp = 4$.

The complexity of the frequency domain calibration is therefore influenced by the number of subcarriers. Complexity of the time domain scheme on the other hand remains constant. As mentioned before, it is also possible to reduce the number of required channel estimates in time-domain calibration. This advantage can be exploited in order to reduce the duration of the calibration process.

VI. Conclusions

In this paper, we have proposed a novel MIMO/TDD uplink downlink reciprocity calibration approach calibrating for the time-domain channel. Simulation results show that the time domain calibration allows to restore the calibration parameters in a MIMO delay spread channel even when antennas are mutual coupled. We applied the scheme to an OFDM system with 512 subcarriers and observed that the new scheme leads to reduced calibration duration and the computation complexity compared to per subcarrier calibration. In order to assess reliability of calibration algorithms and their applicability to over the air links, implementation in a real experimental MIMO-OFDM platform (http://www.openairinterface.org/) are under investigation.

References

[1] The CROWN website, "http://www.fp7-crown.eu/," .

[2] J. Mitola III, "Cognitive Radio Architecture," *Cognitive Radio, Software Defined Radio, and Adaptive Wireless Systems*, pp. 43–107, 2007.

[3] A. Goldsmith, S.A. Jafar, I. Maric, and S. Srinivasa, "Breaking spectrum gridlock with cognitive radios: An information theoretic perspective," *Proceedings of the IEEE*, vol. 97, no. 5, pp. 894–914, 2009.

[4] B. Kouassi, I. Ghauri, B. Zayen, and L. Deneire, "On the performance of calibration techniques for cognitive radio systems," in *The 14th International Symposium WPMC'11*, Brest, France, Oct. 2011.

[5] F. Negro, I. Ghauri, and D.T.M. Slock, "Transmission techniques and channel estimation for spatial interweave TDD cognitive radio systems," in *Signals, Systems and Computers, 2009 Conference Record of the 43rd Asilomar Conf. on*, nov. 2009, pp. 523–527.

[6] M. Guillaud, D.T.M. Slock, and R. Knopp, "A practical method for wireless channel reciprocity exploitation through relative calibration," *8th ISSPA 2005, Sydney, Australia*, pp. 403–406, Aug. 29-Sep. 1,2005.

[7] K.W. Park and Y.S. Cho, "An mimo-ofdm technique for high-speed mobile channels," *IEEE Communications Letters*, vol. 9, no. 7, pp. 604–606, 2005.

[8] F. Kaltenberger, H. Jiang, M. Guillaud, and R. Knopp, "Relative channel reciprocity calibration in mimo/tdd systems," in *Future Network and Mobile Summit, 2010*.

[9] M. Petermann, M. Stefer, D. Wübben, M. Schneider, and K.D. Kammeyer, "Low-complexity calibration of mutually coupled non-reciprocal multi-antenna OFDM transceivers," in *7th ISWCS, 2010*, pp. 285–289.

[10] P. Zetterberg, "Experimental investigation of tdd reciprocity-based zero-forcing transmit precoding," *EURASIP Journal on Advances in Signal Processing*, vol. 2011, pp. 5, 2011.

[11] T.K. Paul and T. Ogunfunmi, "Wireless lan comes of age: Understanding the ieee 802.11n amendment," *IEEE Circuits and Systems Magazine*, vol. 8, no. 1, pp. 28–54, quarter 2008.

[12] I. Markovsky and S. Van Huffel, "Overview of total least-squares methods," *Signal processing*, vol. 87, no. 10, pp. 2283–2302, 2007.

[13] N. Mastronardi, P. Lemmerling, and S. Van Huffel, "Fast structured total least squares algorithm for solving the basic deconvolution problem," *SIAM Journal on Matrix Analysis and Applications*, vol. 22, pp. 533, 2000.

[14] J. Tesic, "Evaluating a class of dimensionality reduction algorithms," .